Effect of aromatic oil on the S-SBR/BR blend components revealed using BDS and PALS

A. RATHI[1#], M. ELSAYED[2,3], R. KRAUSE-REHBERG[2], W.K. DIERKES[1], J. W. M. NOORDERMEER[1], C. BERGMANN[4], J. TRIMBACH[4] and A. BLUME[1]

The focus of this research is on the aromatic process oil, which works as a i) plasticizer thereby decreasing mixing torque and the production cost of the final compound; ii) extender of free volume in the compound so that lesser amount of polymer is needed for the final compound. The precise mechanism of action of the oil to achieve this is still unclear. Therefore, the aim here is to understand the influence of mineral-based aromatic process oil (0-20 phr) on the S-SBR/BR blends in terms of its plasticization and extension behavior. The plasticization behavior is revealed based on the change in glass transition temperature (T_g) studied with Broadband Dielectric Spectroscopy (BDS). While the extension behavior is explored based on changes in fractional free volume investigated with Positron Annihilation Lifetime Spectroscopy (PALS). The BDS analysis leads to a clearer understanding of the plasticization behavior of the oil by studying the change in T_g of each blend component. This is further supported with PALS results which verify the validity of the extension of the free volume associated with the plasticization of each blend component.

Keywords: Aromatic process oil, S-SBR/BR blends, T_g, Free volume

1 Dept. of Elastomer Technology and Engineering, University of Twente, P.O. Box 217, 7500 AE Enschede, The Netherlands
2 Department of Physics, Martin Luther University Halle, 06099 Halle, Germany
3 Department of Physics, Faculty of Science, Minia University, 61519 Minia, Egypt
4 Hansen & Rosenthal KG, Am Sandtorkai 64, 20457 Hamburg, Germany
A. RATHI (e-mail: a.rathi@utwente.nl)

INTRODUCTION

S-SBR (Solution Styrene Butadiene copolymer) / BR (Butadiene homopolymer) blends are widely used for passenger car tire tread applications. The tread compounds are composed of the constituting polymers: S-SBR and BR, a process oil, a filler and a vulcanization system. The polymers S-SBR and BR are chosen for the tire tread compound to achieve a good balance in the overall performance based on the Rolling Resistance (RR), Wet Skid Resistance (WSR) and Abrasion Resistance (AR). High molecular weight S-SBR gives the tread compound a good WSR, while BR gives it a good AR and RR [1-3]. A process oil is an inevitable component in the formulation as it acts as a plasticizer and an extender. It confers numerous advantages to the compound; for example, reduction of compound viscosities, improving homogeneity of rubber mixes due to its plasticization ability; decreasing polymer consumption and increasing filler loading due to its ability to extend the free volume within the polymers. This reduces the mixing energy as well as the polymer consumption thereby reducing the cost to performance ratio of the final compound. A filler imparts the required strength properties to the compound. A crosslinking system is also an imperative component as it makes the bridge like links between the polymer chains which act as the memory sites. These memory sites help the stretched polymer chains to come back to their original position after they have been stretched[4].

Since the European Commission regulation (EC) No. 552/2009 on limiting the use of aromatic oil rich in Polycyclic Aromatic Hydrocarbons (PAHs) in rubber compounds, there was a shift to 'safe' aromatic process oils, which contain lower amounts (<10 mg/kg of the eight listed carcinogenic PAHs) of PAHs [5]. Since 2010, all tire manufacturing companies had to replace the most commonly used Distillate Aromatic Extract (DAE) oils with the new generation of 'safe' process oils such as Treated Distillate Aromatic Extract (TDAE), Mildly Extracted Solvate (MES), Residual Aromatic Extract (RAE) and Naphthenic oil (NAP) for the European market based on the legislative regulation. Amongst those, TDAE is the most commonly used in the S-SBR/BR tread compounds. Therefore, in this work S-SBR/BR (50/50 wt. ratio) blends with 0-20 phr TDAE oil are studied to get a better understanding of the plasticization and extension effect of the oil on each blend component.

This aim is sub-divided into the following questions which will be answered herein:

    i)   How is the T_g of each blend component influenced by addition of TDAE?
    ii)   Is there a preference of the TDAE for one of the blend components?
    iii)   Is the influence on the T_g by the TDAE in agreement with the free volume theory?

In order to answer these questions the following approach was used here. A combination of Broadband Dielectric Spectroscopy (BDS) and Positron Annihilation Lifetime Spectroscopy (PALS) was adapted to reveal the effect of the addition of TDAE oil on these blends. BDS is a specialized technique that measures the complex dielectric permittivity of a material over a wide range of frequencies and temperatures, which allows the accurate detection of very subtle changes in effective T_g's of each blend component [6-13]. A change in glass transition temperature (T_g) upon addition of TDAE is measured using BDS which is taken as an indicator of plasticization efficiency [14]. The degree of change in T_g is used as the parameter to evaluate the preference of the TDAE for either blend component. PALS is an indirect measurement of the fractional free volume (F_v) which identifies the effective T_g's based on the changes in the F_v with temperature [15-21]. PALS is used to analyze the F_v associated with the effective T_g's

of each blend component with regard to the free volume theory governing the extender molecules [22].

MATERIALS AND METHODS

Materials

The materials used in this study are S-SBR: SPRINTAN™ SLR 4602 (Trinseo Deutschland GmbH, Schkopau, Germany); BR: BUNA CB24 (Arlanxeo Deutschland GmbH, Leverkusen, Germany) and Treated Distillate Aromatic Extract (TDAE): VIVATEC 500 (Hansen & Rosenthal KG, Hamburg, Germany). Some analytical properties of S-SBR, BR and TDAE are presented in Table 1. Zinc oxide (ZnO), stearic acid (SA) and sulfur (S) were obtained from Sigma Aldrich (St. Louis, USA), and N-cyclohexyl-2-benzothiazole sulfenamide (CBS) were obtained from Flexys (Brussels, Belgium). All chemical reagents were used as received.

TABLE 1. Reported properties of S-SBR, BR and TDAE oil.

	S-SBR	BR	TDAE
Styrene (wt%)	21	-	-
1,2-vinyl butadiene (%)	50	<1	-
cis-1,4 butadiene (%)	29[a)]	>96	-
trans-1,4 butadiene (%)		~2	-
Weight average molecular weight (M_w)(kg.mol^{-1})	475	460	-
Number average molecular weight (M_n)(kg.mol^{-1})	315	135	-
Glass transition temperature (T_g) (^{o}C)	-25	-109	-49

[a)] 29% is the combined contribution of cis-1,4 and trans-1,4 in the S-SBR microstructure

Mixing

The basic formulation used for this study is presented in Table 2, expressed in parts per hundred parts of rubber (phr). The compounds were prepared following a 2-step mixing procedure, with a first stage in an internal mixer. The vulcanization system (CBS+S) was added to the mix in a second stage, carried out on a two-roll mill: Table 3. The compounds are referred to as S-SBR/BR_x phr, where "x" corresponds to the amount of TDAE added to the formulations (0/10/20 phr).

TABLE 2. Rubber Formulations.

Component	S-SBR/BR (phr)
BR	50
S-SBR	50
Zinc Oxide (ZnO)	4
Stearic Acid (SA)	3
N-cyclohexyl-2-benzothiazole sulfenamide (CBS)	2.5
Sulfur (S)	1.6
Treated Distillate Aromatic Extract (TDAE)	0/10/20

Curing

The samples were vulcanized in a hydraulic press (Wickert WLP 1600) at 100 bar and 160 °C as sheets with a thickness of 2 mm, according to their $t_{c,90}$ + 2 mins optimum vulcanization times: see Table 4. The $t_{c,90}$ was determined with a Rubber Process Analyzer (RPA 2000, Alpha Technologies) following ISO 3147:2008 at 160 °C. 0.1-0.2 mm thick sheets were also vulcanized according to their respective $t_{c,90}$ values at 160 °C for BDS measurements.

TABLE 3. Mixing Protocol.

1st Stage: Internal Mixer Brabender Plasticorder 350S Rotor speed: 50 RPM; Set temperature: 50 °C; Fill factor: 0.7			**2nd Stage: Two-roll mill Polymix 80T Friction ratio: 1.25:1; ca. 40°C**
S-SBR/BR_0 (min. sec.)	**S-SBR/BR_10** (min. sec.)	**S-SBR/BR_20** (min. sec.)	**All compounds** (min. sec.)
0.30 Add Polymers	0.30 Add Polymers	0.30 Add Polymers	0.30 Add Curatives (CBS+S)
1.30 Add ZnO and SA	1.30 Add ZnO and SA	1.30 Add ZnO and SA	5.00 Discharge
4.00 Discharge	2.40 Add 3/4th TDAE	2.40 Add 3/8th TDAE	
	5.00 Add 1/4th TDAE	5.00 Add 3/8th TDAE	
	7.00 Discharge	8.00 Add 1/4th TDAE	
		10.30 Discharge	

Broadband Dielectric Spectroscopy

Broadband Dielectric Spectroscopy (BDS) measurements were performed on a spectrometer with an ALPHA-A High Performance Frequency Analyzer (Novocontrol Technologies). The vulcanized 0.1-0.2 mm sheets were cut in a disk shape and were mounted in the dielectric cell between two parallel gold plated electrodes. The complex dielectric permittivity ε^* ($\varepsilon^* = \varepsilon' - i\varepsilon''$), being composed of ε' as the real part and ε'' the imaginary part, was measured by performing consecutive isothermal frequency sweeps (10^{-1}-10^6 Hz) in the temperature range from -120 °C to +80 °C in steps of 5 °C. The temperature was controlled to $\pm$ 0.1 °C with a Novocontrol Quatro cryosystem; the error of the ALPHA impedance measurement was less than 1%.

Positron Annihilation Lifetime Spectroscopy

The positron annihilation lifetime spectroscopy (PALS) measurements were performed using a digital lifetime spectrometer with a time resolution of 170 ps [23], where a 740 kBq ^{22}Na positron source protected by 7.5 μm thick Kapton foil was sandwiched between two identical samples each 1.5 mm thick. This arrangement was wrapped in Al-foil and placed in the sample holder. The samples were measured in the temperature range of -140 to +60 °C. 5×10^6 counts were accumulated in each positron lifetime spectrum.

RESULTS AND DISCUSSION

Broadband Dielectric Spectroscopy (BDS)

Havriliak-Negami (HN) analysis of blends

Broadband Dielectric Spectroscopy (BDS) measures complex dielectric permittivity of a material in the frequency as well as the temperature domain. The frequency-domain dielectric data can be analyzed by fitting the complex dielectric function $\varepsilon^*(\omega)$ with empirical relaxation functions of the Havriliak-Negami (HN) type. The HN equation is a phenomenological expression which can describe a dielectric relaxation process in terms of a characteristic relaxation time at the frequency of the maximum loss [24]. It reads as follows:

$$\varepsilon^*_{HN}(\omega) = \varepsilon_\infty + \frac{\Delta\varepsilon}{[1+(i\omega\tau_{HN})^b]^c} \qquad (1)$$

where τ_{HN} is the characteristic HN relaxation time, which represents the most probable relaxation time from the relaxation time distribution function, ω is the angular frequency, $\Delta\varepsilon$ is the relaxation strength ($\Delta\varepsilon = \varepsilon_s - \varepsilon_\infty$), where ε_∞ and ε_s are related to the limiting behavior of the complex dielectric function at low and high frequencies respectively, $\varepsilon^*_{HN}(\omega)$ is the frequency dependent Havriliak-Negami complex dielectric permittivity, and b and c are shape parameters, which describe the symmetric and asymmetric broadening of the relaxation time distribution function, respectively.

Blending modifies the response of the individual S-SBR and BR components such that they may experience a distinct relaxation environment in the blended state, which can be fitted as individual contributions [25]. The experimental ε'' versus frequency spectra for the S-SBR/BR blends with and without oil obtained from BDS were fitted using two HN equations in order to resolve the individual contributions of the S-SBR and BR components from the single, broad dielectric loss ε'' peak of the blends [25, 26]. The fittings were performed with the aim of finding

two relaxation processes which are referred to as α for a fast and α' for a slow process. At a selected temperature T= -30 °C the dielectric loss ε″ is clearly observable as a well-resolved peak of about six decades in the frequency window: Figure 1. The dielectric loss ε″ de-convoluted into two individual relaxation processes depicted as dashed lines. A conductivity contribution, shown as dotted line, was used in the fitting protocol to achieve a better fit of the low frequency tail of the dielectric spectra. The α and α′ relaxations are assigned as the fast and the slow process, respectively, in decreasing order of frequency, related to a BR-rich and a blend-rich environment [27].
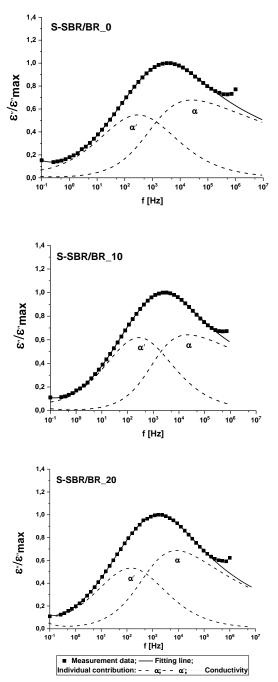

FIGURE 1. Normalized deconvolution results from fitting of the α′ and α processes using 2 HN equations at T = -30 °C for the blends: S-SBR/BR_0, S-SBR/BR_10, and S-SBR/BR_20.

The relaxation parameters: $\Delta\varepsilon_{(\alpha)}$, $\Delta\varepsilon_{(\alpha\prime)}$, b, b′, c, c′, $\tau_{HN(\alpha a)}$, and $\tau_{HN(\alpha a\prime)}$ (where ′ refers to the α'-process) for each contribution are shown in Table 4 for selected temperatures of -40, -30

and -20 °C. τ_{HN} is related to the relaxation time of maximum loss, τ_{max} and the frequency of maximum loss, f_{max} by the following equation [28]:

$$\tau_{max} = \frac{1}{2\pi f_{max}} = \tau_{HN} \left[\sin \frac{b\pi}{2+2c} \right]^{-\frac{1}{b}} \left[\sin \frac{bc\pi}{2+2c} \right]^{\frac{1}{b}} . \qquad (2)$$

The corresponding values of τ_{max}, plotted in Figure 2, reveal the Vogel-Fülcher-Tamman (VFT) dependence of τ_{max} on the reciprocal temperature as [29-31]:

$$\tau_{max} = \tau_0 \exp\left(\frac{B}{T - T_0}\right) \qquad (3)$$

where τ_0 and B are empirical parameters, and T_0 is called the ideal glass transition or Vogel temperature, which is generally 30-70 K below T_g [29]. A universal value of $\log \tau_0 = -14$ was adapted for the data fitting using the VFT equation, based on the relationship of τ_0 with the C_1 (~17) universal parameter from the WLF equation [32].

TABLE 4. HN-fitting parameters for the de-convoluted relaxation spectra of S-SBR/BR blends with varying concentrations of TDAE.

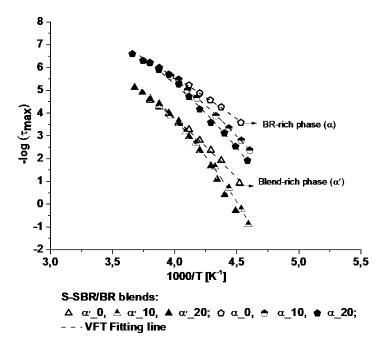| Compound	S-SBR/BR_0	S-SBR/BR_10	S-SBR/BR_20
T = -40 °C			
$\Delta\varepsilon_\alpha$	0.22	0.60	0.24
$\Delta\varepsilon_{\alpha'}$	0.11	0.24	0.18
τ_{HN} (α) (s)	1.14×10^{-3}	1.71×10^{-3}	1.85×10^{-3}
τ_{HN} (α′) (s)	6.31×10^{-3}	1.67×10^{-2}	1.91×10^{-2}
B	0.58	0.54	0.53
b′	0.38	0.22	0.39
C	0.11	0.42	0.19
c′	1	0.97	0.80
T = -30 °C			
$\Delta\varepsilon_\alpha$	0.25	0.64	0.26
$\Delta\varepsilon_{\alpha'}$	0.09	0.26	0.16
τ_{HN} (α) (s)	1.52×10^{-4}	1.51×10^{-4}	1.76×10^{-4}
τ_{HN} (α′) (s)	5.87×10^{-4}	8.68×10^{-4}	9.56×10^{-4}
B	0.63	0.65	0.65
b′	0.44	0.49	0.44
C	0.11	0.14	0.15
c′	1	0.90	0.89
T = -20 °C			
$\Delta\varepsilon_\alpha$	0.27	0.72	0.30
$\Delta\varepsilon_{\alpha'}$	0.07	0.20	0.12
τ_{HN} (α) (s)	2.49×10^{-5}	3.30×10^{-5}	3.59×10^{-5}
τ_{HN} (α′) (s)	9.30×10^{-5}	1.18×10^{-4}	1.44×10^{-4}
B	0.71	0.73	0.72
b′	0.52	0.53	0.53
C	0.10	0.12	0.14
c′	1	1	0.96

FIGURE 2. Temperature dependence of the average relaxation times of: TDAE; α and α' processes for the blends: S-SBR/BR_0, S-SBR/BR_10, and S-SBR/BR_20.

TABLE 5. T_g^{eff} at τ_{max}=100 s and 1 s of the α and α' processes, experimentally obtained from BDS measurements.

Compound	α (BR-rich phase) / α' (Blend-rich phase)	T_g^{eff} (100 s) (°C)	ΔT_g^{eff} (100 s) (°C)
S-SBR/BR_0	α	-97	-
	α'	-72	-
S-SBR/BR_10	α	-80	17
	α'	-61	11
S-SBR/BR_20	α	-75	22
	α'	-59	13

NOTE: ΔT_g^{eff} is calculated with regard to S-SBR/BR_0.

Figure 2 shows τ_{max} for the BR-rich (α) and Blend-rich (α') relaxation process plotted as a function of the inverse temperature. The relaxation time curves of the two processes are located apart from each other and seem to converge at higher temperatures. This trend is observed independent of the amount of oil present in the blends as at higher temperature the dielectric relaxation time reaches a limit of $\tau_\infty \cong 10^{-13}$ s which is corresponding to local orientational fluctuations [33]. The effective T_g (T_g^{eff}) of the fast and the slow process in the blend are subsequently calculated as the temperature at the conventional τ_{max}=100 s (~10^{-2} Hz), as listed in Table 5 [34]. Upon addition of oil, the observed trend is that both the BR-rich and blend-rich processes show longer relaxation times with increasing amounts of oil, which can be expected since the TDAE oil has slower relaxation dynamics compared to the blends due to the steric hindrances from the bulky naphthenic and aromatic rings. This effect can most clearly be seen in Figure 2. A clear shift towards higher T_g^{eff} for both the BR-rich and blend-rich processes is observed as the oil content increases, the degree of shift being more pronounced for the BR-rich process as compared to the blend-rich process: see Table 6. This shows that the BR-rich

process is more plasticized as compared to the blend-rich process. The faster BR-rich process originates from the relaxation of BR segments surrounded predominantly by like-segments and oil. Hence, the BDS method successfully answers the questions of which blend component is influenced to what extent. A more in-depth explanation of the reason behind the preference of TDAE oil for the BR-rich process is that the inherent free volume associated with BR due to its linearity is smaller compared to that of S-SBR due to the bulky styrene-groups and variety of microstructures, which means that addition of TDAE oil causes a higher disruption in the relaxation dynamics of BR, whereas in the case of S-SBR most of the TDAE oil can accommodate in the existing free volume without causing much differences to its relaxation dynamics. This explains why a relatively bigger effect of the oil can be noted for the BR-rich process on Table 5. To further examine this idea in terms of changes in free volume with the addition of TDAE oil, a PALS based approached is applied in this research. The details of the PALS based approach are described in the following section.

Positron Annihilation Lifetime Spectroscopy (PALS)

Positron Annihilation Lifetime Spectroscopy (PALS) generates a counts versus time spectra by detecting the time between generation and annihilation of the positron. The raw positron lifetime spectra are corrected for source as well as background and analyzed by the lifetime LT 9 program [35]. The lifetime spectra are then resolved into three components τ_1, τ_2 and τ_3 with corresponding intensities I_1, I_2 and I_3. The shortest lifetime τ_1=0.12-0.15 ns with intensity I_1 is the response from *para*-Positronium (*p*-Ps) and free positron annihilations. The second lifetime τ_2=0.33-0.40 ns with intensity I_2 is the response from annihilation of positrons trapped at the defects present in the material. The third lifetime τ_3=1-3 ns with intensity I_3 is the longest component arising from pick-off annihilation of the *ortho*-Positronium (*o*-Ps) from the free volume holes in the amorphous region of the polymer. The o-Ps lifetime can be related to the radius R of the free volume using the Tao-Eldrup model which assumes the free volume holes to be spherical.

$$\tau_{o-Ps} = 0.5 \text{ ns} \left[\frac{\Delta R}{R + \Delta R} + \frac{1}{2\pi} \sin\left(2\pi \frac{R}{R + \Delta R}\right) \right]^{-1}$$

Where τ_{o-Ps} is the lifetime of o-Ps, R is radius of free volume hole and ΔR is the electron-rich layer where the pick-off annihilation takes place. ΔR is conventionally taken as 0.166 nm. This allows the monitoring of the changes in the average volume of holes V_h (=$4/3\pi R^3$) associated with the glass-to-rubber transition on a temperature scale. The V_h derived from τ_3 can also be combined with I_3 to give fractional free volume (F_v), which is expressed as the following relation:

$$F_v = A \times V_h \times I_3$$

Where V_h (in Å^3) is the free volume of the holes calculated using R from the Tao-Eldrup model, I_3 (in %) is its intensity and A is a proportionality constant that is determined to be 0.0018 from specific volume data for polymers [15]. F_v is expressed in % and does not have the physical units of volume [18].

The point of change in the slope in the F_v vs temperature curves is taken as the glass transition temperature (T_g). In Fig 3 it can be seen that there are two major changes in the slope: one is at lower temperature and the other one is at much higher temperature (~20 °C). The lower one is

conventionally accepted as the T_g^{PALS} and the higher one is taken as the saturation temperature (T_s) [17]. The reduced slope of F_v above T_s is either due to the fact that the matrix is too soft and hence the *o*-Ps cannot find rigid walls around it or it is due to the fact that τ_3 becomes comparable to the relaxation time of molecular chains. In the current system with S-SBR/BR (50/50) blends the T_s is around 20 °C. Ideally, in the range between the T_g^{PALS} and T_s the temperature-dependent *o*-Ps lifetime is a linear function in the fully amorphous systems [17]. However, in the case of blends an additional bending temperature is observed. This bending temperature is above the T_g of BR and lower than T_g of S-SBR, which means that it should be a contribution of the blend consisting of both S-SBR and BR chains. In other words, the T_g^{eff} corresponding to the BR-rich phase and the blend-rich phase can be identified on these curves. This supports the BDS results as well as gives an insight about the respective changes in the fractional free volume associated with the T_g^{eff} of the BR-rich process and the blend-rich process. A detailed consideration of the changes on the F_v with addition of TDAE oil shows that the F_v increases steadily for both the BR-rich as well as the blend-rich process. According to the free volume theory of plasticization, low molecular weight molecules like TDAE oil have the effect of pushing the polymer chains apart, effectively increasing in this way the free volume. The TDAE oil is composed of paraffinic, naphthenic and aromatic molecules. Even though the TDAE oil has a lower molecular weight compared to S-SBR and BR, the variety of molecules present in the oil especially aromatic molecules being bulky molecules can effectively increase the distance between the polymer chains due to steric hindrance. This effectively increases the free volume in a compound. The increase in free volume of both the BR-rich and the blend-rich process on addition of TDAE oil is in accordance with the free volume theory of plasticization as it proves the extension effect of the oil within the S-SBR/BR blends. Hence, it also answers the third question in the current research by verifying the role of the free volume theory of plasticization in change in T_g^{eff}'s of the BR-rich and the blend-rich process on addition of TDAE oil.
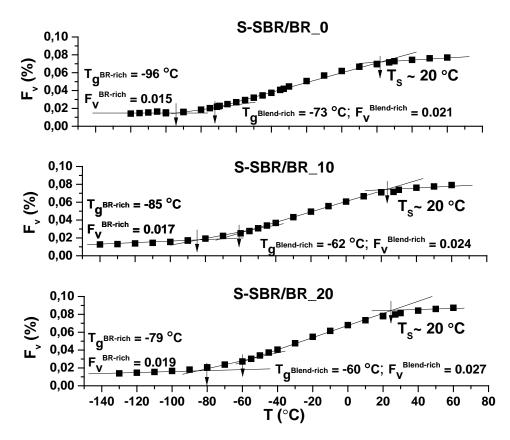
FIGURE 3. Fractional free volume F_v as a function of temperature for S-SBR/BR_0, S-SBR/BR_10 and S-SBR/BR_20.

CONCLUSIONS

In this study, S-SBR/BR (50/50) blends with and without TDAE oil were investigated. The effect of the TDAE oil on the T_g^{eff} of each blend component was studied using BDS, while the mechanism of the observed effect was deciphered using PALS to probe the free volume changes. From the BDS measurements, a combined dielectric loss ε'' was observed for the compounds. It could be deconvoluted using a HN-fitting protocol into a BR-rich process and a blend-rich process. The corresponding T_g^{eff}'s of the identified blend components $T_g^{BR-rich}$ and $T_g^{blend-rich}$ were then examined for the effect of TDAE oil. A larger shift is observed on the $T_g^{BR-rich}$ on addition of 10 and 20 phr of TDAE oil compared to that on $T_g^{Blend-rich}$. It indicates a better plasticization as well as preference of the TDAE oil for the BR-rich component. In order to elucidate the mechanism behind this effect, the compounds were further studied with PALS to see the changes in the free volume associated with the shift in T_g^{eff} of the BR-rich and blend-rich components. The PALS measurements supported the T_g^{eff} values obtained from BDS measurements. The mechanism of plasticization could be clarified from the fractional free volume data that is obtained from PALS. A steady increase in the fractional free volume (F_v) of the BR-rich and Blend-rich components was observed with the addition of 10 and 20 phr TDAE. This confirmed the extension effect of the TDAE oil on both BR-rich and blend-rich processes as well as validated the applicability of the free volume theory of plasticization in this case.

11

REFERENCES

[1] J. Fujimoto, N. Yoshimiya, Rubber Chem. Tech. **1968**, 41, 669.
[2] N. Yoshimiya, J. Fujimoto, Rubber Chem. Tech. **1969**, 42, 1009.
[3] T. Inoue, F. Shomura, T. Ougizawa, K. Miyasaka, Rubber Chem. Tech. **1985**, 58, 873.
[4] H. W. Engels, et al., Rubber, 9. Chemicals and Additives, in Ullmann's Encyclopedia of Industrial Chemistry, Wiley-VCH Verlag GmbH & Co. KGaA: Weinheim, DE, **2011**
[5] EU, *Directive 2005/69/EC of the European Parliament and of the Council*, in *323*, O.J.o.E. Union, Editor. 2005.
[6] S. Shenogin, R. Kant, R.H. Colby, S.K. Kumar, Macromolecules **2007**, 40, 5767.
[7] Y. Hirose, O. Urakawa, K. Adachi, Macromolecules **2003**, 36, 3699.
[8] S.A. Madbouly, Polymer **2002**, 34, 515.
[9] J. Colmenero, A. Arbe, Soft Matter **2007**, 3, 1474.
[10] W.G.F. Sengers, M. Wübbenhorst, S.J. Picken, A.D. Gotsis, Polymer **2005**, 46, 6391.
[11] D. Boese, F. Kremer, Macromolecules **1990**, 23, 829.
[12] B.B. Sauer, P. Avakian, G.M. Cohen, Polymer **1992**, 33, 2666.
[13] S. Cerveny, R. Bergman, G.A. Schwartz, P. Jacobsson, Macromolecules **2002**, 35, 4337.
[14] Hiemenz, P.C., *The Glassy and Crystalline States*, in *Polymer Chemistry: The Basic Concepts*, P.C. Hiemenz, Editor. 1984, Marcel Dekker, Inc.: New York, U.S.
[15] J. Liu, Y.C. Jean, H. Yang, Macromolecules **1995**, 28, 5774.
[16] G.N. Kumaraswamy, C. Ranganathaiah, M.V. Deepa Urs, H.B. Ravikumar, European Polymer Journal **2006**, 42, 2655.
[17] W. Salgueiro, A. Somoza, L. Silva, G. Consolati, F. Quasso, M.A. Mansilla, A. J. Marzocca, Physical Review E **2011**, 83, 051805.
[18] A.J. Hill, M.D. Zipper, M.R. Tant, G.M. Stack, T.C. Jordan, A.R. Shultz, J. Phys.: Condens. Matter **1996**, 8, 3811.
[19] D. Račko, R. Chelli, G. Cardini, J. Bartoš, S. Califano, Eur. Phys. J. D **2005**, 32, 289.
[20] Y. Zhu, W. Zhou, J. Wang, B, Wang, J. Wu, G. Huang, J. Phys. Chem. B **2007**, 111, 11388.
[21] R. Srithawatpong, Z.L. Peng, B.G. Olson, A. M. Jamieson, R. Simha, J.D. McGervey, T.R. Maier, A. F. Halasa, H. Ishida, Journal of Polymer Science: Part B: Polymer Physics **1999**, 37, 2754.
[22] Cadogan, D.F. and C.J. Howick, *Plasticizers*, in *Ullmann's Encyclopedia of Industrial Chemistry*, Wiley-VCH Verlag GmbH & Co. KGaA: Weinheim, DE, **2012**
[23] O. Hauenstein, M.M. Rahman, M. Elsayed, R. Krause-Rehberg, S. Agarwal, V. Abetz, and A. Greiner, Adv. Mater. Technol. 2**017**, 1700026
[24] S. Havriliak, S. Negami, Polymer **1967**, 8, 161.
[25] S. Zhang, P. Painter, J. Runt, Macromolecules **2002**, 35, 9403.
[26] M. Hernández, T.A. Ezquerra, R. Verdejo, M.A. López-Manchado, Macromolecules **2012**, 45, 1070.
[27] A. Rathi, M. Hernández, S.J. Garcia, W.K. Dierkes, J.W. M. Noordermeer, C. Bergmann, J. Trimbach, A. Blume, Journal of Polymer Science: Part B: Polymer Physics **2018**, 56, 842.
[28] R. Richter, C.A. Angell, J. Chem. Phys. **1998**, 108, 9016.
[29] H. Vogel, Phys. Z. **1921**, 22, 645.

[30] G.S. Fülcher, J. Am. Cer. Soc. **1925**, 8, 339.

[31] G. Tammann, W. Hesse, Z. Anorg. Allg. Chem. **1926**,156, 245.

[32] C.A. Angell, Polymer **1997**, 38, 6261.

[33] Kremer F., Schönhals A., *The Scaling of the Dynamics of Glasses and Supercooled Liquids*, in *Broadband Dielectric Spectroscopy*, F. Kremer, A. Schönhals, Editors, Springer-Verlag: Berlin Heidelberg, Germany, **2003**

[34] C.A. Angell, J. Non-Crystalline Solids **1991**, 131, 13.

[35] J. Kansy, Nucl. Instrum. Methods A **1996**, 374, 235.